

Thermal Ising transition in two-dimensional SU(3) Fermi lattice gases with population imbalance

Hayato Motegi,¹ Giacomo Marmorini,^{1,2} Nobuo Furukawa,¹ and Daisuke Yamamoto^{2*}
¹*Department of Physics and Mathematics, Aoyama Gakuin University, Sagamihara, Kanagawa, Japan*
²*Department of Physics, Nihon University, Tokyo, Japan*

We focus on three-component SU(3) Fermi gases loaded into a square optical lattice, with population imbalance between one component and the others. At strong coupling the system is described by the SU(3) Heisenberg model with an external field that couples to the population imbalance. We discuss the ground state at the mean-field level and then analyze the thermal fluctuations with the semi-classical Monte-Carlo method. The interplay of interactions, population imbalance and thermal fluctuations gives rise to a phase transition linked to the breaking of an emergent Ising symmetry, despite the absence of frustration. This represents a new scenario of discrete symmetry breaking in low-dimensional systems with continuous symmetries. Possible implementations with cold alkaline-earth(-like) atoms are discussed.

Introduction.— Symmetry and its spontaneous breaking have been playing a central role for understanding the low-energy physics of many-body systems and classifying phase transition phenomena. According to the Mermin-Wagner-Hohenberg theorem [1, 2], continuous symmetries cannot be spontaneously broken at nonzero temperature in one and two-dimensional systems with sufficiently short-range interactions. However, it has been found in certain systems with only continuously symmetric interactions that a spontaneous symmetry breaking with respect to a discrete order parameter can emerge through a nontrivial mechanism even in low dimensions at nonzero temperature. In the framework of Heisenberg-like models, in a seminal work [3] Chandra, Coleman and Larkin introduced the idea that this scenario can be realized in the presence of frustration coming from competing exchange interaction; in fact, their proposal of an Ising transition in the frustrated J_1 - J_2 model on the square lattice has been confirmed in various subsequent studies [4–6]. An additional example of this kind is given by the Ising transition in the fully frustrated spin-1/2 Heisenberg ferromagnetic/antiferromagnetic square bilayer [7, 8]. In the triangular lattice Heisenberg model it is the interplay of geometric frustration and magnetic field that stabilizes the up-up-down state, which breaks only a discrete translational Z_3 symmetry. In this Letter we aim to extend these concepts to SU(\mathcal{N})-symmetric Heisenberg models: we argue that, even without frustration coming from geometry or competing exchange interactions, the presence of a suitable “external field” (the SU(\mathcal{N}) symmetry admits $\mathcal{N} - 1$ couplings that play the role of generalized magnetic fields) can indeed induce the breaking of an emergent discrete symmetry.

Due to the high controllability of various parameters including interaction, dimensionality, and population of particles, ultracold-atom experiments provide an ideal platform for quantum simulation of many-body physics. For instance, two-component Fermi atoms in an optical lattice can realize the Hubbard model [9] — the simplest

model for strongly correlated electrons. At half filling and strong coupling the system is well approximated by the SU(2) Heisenberg model [10] and, for bipartite lattices in two or more dimensions, the ground state is the conventional antiferromagnetic state. Recent experiments employing the quantum gas microscope technique have confirmed that in a square optical lattice the spin-spin correlation function does not exhibit true long-range order and decays exponentially with distance, as expected at low but finite temperatures ($\gtrsim 0.25$ times the tunnelling energy) [9]. Thanks to the advances in the manipulation of cold alkaline-earth(-like) atoms, such as ^{173}Yb and ^{87}Sr , analogous experiments on systems with SU(\mathcal{N}) symmetry, $\mathcal{N} > 2$, have been underway [11, 12]. This has stimulated vast theoretical work, leading to numerous predictions of exotic ground states for various lattice geometries and degrees of freedom \mathcal{N} [13–15]. However, the effects of thermal fluctuations and “external fields” that partially break the SU(\mathcal{N}) symmetry have been rarely investigated [16]. Note that in cold-atom experiments, such an external-field effect can be simulated by imposing a global imbalance of populations among the \mathcal{N} components [17].

Model.— Inspired by the above considerations, in this work we study the strong coupling regime of three-component Fermi gases with SU(3)-symmetric interactions in a square optical lattice at 1/3 filling [13, 14] with population imbalance between one component and the others, which breaks the original SU(3) symmetry down to SU(2)×U(1). The system is described by the antiferromagnetic SU(3) Heisenberg model with an external field:

$$\hat{\mathcal{H}} = \frac{J}{2} \sum_{\langle i,j \rangle} \hat{\lambda}_i \cdot \hat{\lambda}_j - D \sum_i \hat{\lambda}_{8,i} \quad (J > 0), \quad (1)$$

where $\hat{\lambda}_i = (\hat{\lambda}_{1,i}, \hat{\lambda}_{2,i}, \dots, \hat{\lambda}_{8,i})$ are the generators of the SU(3) Lie algebra in the defining representation [18], acting on the three local basis states, which we refer to as three “colors”, $|\mathbf{R}_i\rangle$, $|\mathbf{B}_i\rangle$, and $|\mathbf{G}_i\rangle$ [13, 14], at site i . In

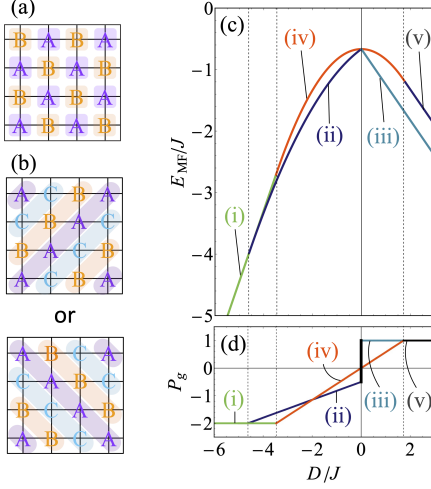


FIG. 1. Illustration of the two and three-sublattice structures with ordering wave vectors (a) $\mathbf{Q}_2 = (\pi, \pi)$ and (b) $\mathbf{Q}_3^+ = (2\pi/3, -2\pi/3)$ or $\mathbf{Q}_3^- = (2\pi/3, 2\pi/3)$. (c) Energy per site and (d) global population imbalance of the mean-field states as functions of the field D at zero temperature.

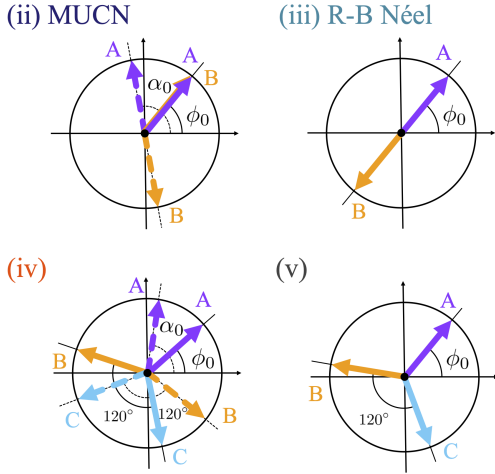


FIG. 2. Two relative phases α_i, ϕ_i in the mean-field states (ii)-(iv) on the corresponding sublattice structures displayed in Figs. 1(a) or (b) in a fixed gauge with $\theta_i = \pi/2$. The angles α_0, ϕ_0 can be arbitrarily chosen independently. In states (iii) and (v), α_i is not defined since $s_i = 1$.

the form given by the Gell-Mann matrices, $\hat{\lambda}_3$ and $\hat{\lambda}_8$ are diagonal, $\text{diag}[1, 0, -1]$ and $\frac{1}{\sqrt{3}}\text{diag}[1, 1, -2]$, respectively, while the others have off-diagonal entries, responsible for the color change of the local state. The last term of Eq. (1) represents a bias field controlling global population imbalance P_g between $\{R, B\}$ and G . Although this partially breaks the original $\text{SU}(3)$, the system still possesses the continuous $\text{SU}(2) \times \text{U}(1)$ symmetry, related to the global rotations in the $\text{SU}(2)$ space generated by $\hat{\lambda}_{1-3}$ and that around $\hat{\lambda}_8$.

The $\text{SU}(3)$ Heisenberg model corresponds to the spin-1 Hamiltonian with equal bilinear and biquadratic exchange couplings [19], which has been discussed in the context of spin liquid in NiGa_2S_4 [20], under the identifications $\{|R_i\rangle, |B_i\rangle, |G_i\rangle\} \mapsto \{|1_i\rangle, |-1_i\rangle, |0_i\rangle\}$. In the language of solid state physics, the imbalance field D corresponds to the intrinsic single-ion anisotropy of the magnetic material. In artificial quantum systems of alkaline-earth(-like) atoms in optical lattices, the Hamiltonian (1) can be realized more directly with no fine-tuning of coupling parameters. Those atoms possess $\text{SU}(2I+1)$ -symmetric repulsive interaction for nuclear spin I ($I = 5/2$ for ^{173}Yb and $I = 9/2$ for ^{87}Sr), and the technique of optical pumping allows for the preparation of any number \mathcal{N} of components out of the $2I+1$ spin states. [21]

The mean-field ground state.— First, we consider the mean-field ground state of Eq. (1) at zero temperature, based on a variational wave function of the form $|\Psi\rangle = \prod_i |\psi_i\rangle$ with $|\psi_i\rangle = d_{R,i}|R_i\rangle + d_{B,i}|B_i\rangle + d_{G,i}|G_i\rangle$. The coefficients can be represented by a normalized complex vector parametrized as

$$\mathbf{d}_i \equiv (d_{R,i}, d_{B,i}, d_{G,i}) = \left(\sqrt{s_i} \cos \frac{\theta_i}{2}, \sqrt{s_i} e^{i\phi_i} \sin \frac{\theta_i}{2}, e^{i\alpha_i} \sqrt{1-s_i} \right). \quad (2)$$

The amplitude and phases $(s_i, \theta_i, \phi_i, \alpha_i) \in [0, 1] \times [0, \pi] \times [0, 2\pi]^2$ should be determined in such a way that the variational energy $E_{\text{MF}} = \langle \Psi | \hat{\mathcal{H}} | \Psi \rangle = J \sum_{\langle i,j \rangle} |\mathbf{d}_i^\dagger \cdot \mathbf{d}_j|^2 - D \sum_i (3s_i - 2)/\sqrt{3}$ is minimized. For $D = 0$, namely at the $\text{SU}(3)$ -symmetric point, the minimization only imposes that the \mathbf{d}_i vectors on neighboring sites are orthogonal. This is not enough to uniquely determine the global configuration of the \mathbf{d}_i vectors, resulting in an accidental ground state degeneracy within the mean-field approximation. Previous studies have predicted that the thermal fluctuations favor the Néel configuration shown in Fig. 1(a) via entropic selection [13, 14], while the three-color stripe long-range order shown in Fig. 1(b) is chosen via a quantum order by disorder mechanism.

In the presence of an imbalance field D , this degeneracy is already lifted without taking fluctuations into account. In Figs. 1(c) and (d), we show the values of the energy per site and the global population imbalance P_g , respectively, as functions of D/J , for several mean-field solutions, labeled (i-v). For $D < 0$, the imbalance field D tends to increase the global population of the $|G\rangle$ state and competes with the antiferromagnetic coupling J , which tends to arrange different colors at neighboring sites. When D is sufficiently negative ($D < -8J/\sqrt{3}$), the forced ferromagnetic state [(i) in Fig. 1] is formed ($|\psi_i\rangle = |G\rangle$ for all i). For $-8J/\sqrt{3} < D < 0$, we found the “minority-united canted-Néel” (MUCN) phase [(ii) in Figs. 1, 2], in which the variational parameters in Eq. (2) are $(s_i, \theta_i, \phi_i, \alpha_i) = (\frac{1}{2} (1 + \frac{\sqrt{3} D}{J}), \theta_0, \phi_0, \mathbf{Q}_2 \cdot \mathbf{r}_i + \alpha_0)$, as

the ground state. Here, the phases θ_0, ϕ_0 , and α_0 are arbitrary and $\mathbf{Q}_2 = (\pi, \pi)$ is the propagation vector. In the MUCN state, while the phase α_i is alternating on the two sublattices (see Fig. 1(a)), interestingly the SU(2) sector of R and B exhibits ferromagnetic order with uniform θ_0 and ϕ_0 , despite the antiferromagnetic nature of the exchange interaction. This can be understood as a mechanism to minimize the interaction energy between the majority G and the minorities {R, B}. Notice that, the MUCN state can be mapped to the conventional canted-Néel state via $\cos(\theta/2)|R\rangle + e^{i\phi}\sin(\theta/2)|B\rangle \mapsto |\uparrow\rangle$, $|G\rangle \mapsto |\downarrow\rangle$. For $D > 0$, since the global population of $\{|R_i\rangle, |B_i\rangle\}$ tends to increase, there is no competition with the antiferromagnetic interactions. Therefore, an infinitesimally small field stabilizes (iii), the standard Néel order (with R and B), which is of course the ground state of the SU(2) Heisenberg model.

Although the mean-field theory predicts the two-sublattice ground states (MUCN and R-B Néel), besides the uniform state for $D < -8J/\sqrt{3}$, we also found three-sublattice solutions as metastable states [corresponding to (iv) and (v) in Figs. 1(c) and (d)]. While in state (iv) the three colors coexists with $r(D < 0) = \frac{1}{2} \left(1 + \frac{1}{\sqrt{3}} \frac{D}{J}\right)$, $r(D > 0) = \frac{1}{2} \left(1 - \frac{1}{2\sqrt{3}} \frac{D}{J}\right)$, the component $|G\rangle$ vanishes in state (v), that is, $s_i = 1$. All these states, including the above-mentioned MUCN and R-B Néel, are massively degenerate, owing to the $SU(2) \times U(1)$ symmetry of the Hamiltonian. Upon choosing the gauge $\theta_i = \pi/2$, for which densities of B and R particles are identical and uniform on the lattice, we summarize the remaining two parameters ϕ and α of the mean-field solutions [(ii)-(v)] in Fig. 2.

Thermal phase diagram.— Since the current experiments have not reached the highly-quantum low-temperature regime yet, addressing the finite temperature effects becomes important beyond a purely theoretical motivation. We hereby take into account thermal fluctuations from the mean-field ground state using semi-classical multi-color Monte-Carlo (sMC) simulations [16, 22].

We perform the standard Metropolis algorithm that allows the complex vectors \mathbf{d}_i on $L \times L$ sites under periodic boundary conditions to fluctuate thermally with the Boltzmann weight $\exp(-E_{\text{MF}}/T)$. In addition, we employ the relaxation acceleration (RA) technique [16]. The single Monte Carlo step consists of the Metropolis updates for $d_{\sigma,i}$ over the entire lattice, followed by double RA sweeps. This procedure can enhance decorrelation and increase the convergence speed [16].

Figure 3 shows the sMC thermal phase diagram. The most surprising feature is a fluctuation-induced phase with true long-range order emerging for $-0.8 \lesssim D < 0$. The R-B Néel and MUCN states, being continuous-symmetry-breaking states, only possess short-range correlations and a crossover connects them to the high-

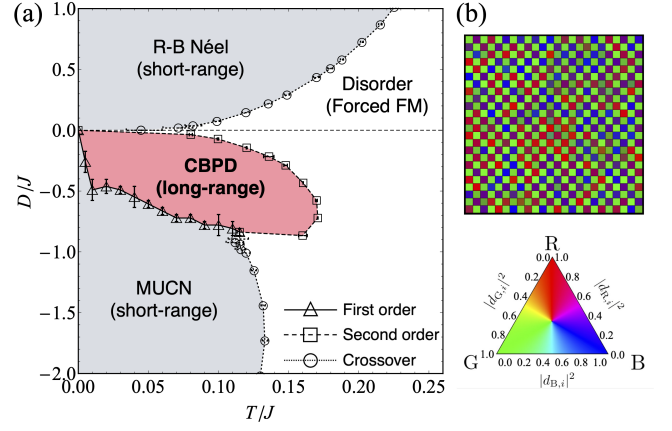


FIG. 3. (a) Thermal phase diagram obtained by the sMC simulations. The crossover temperature T_c^* is determined by the temperature where the correlation length reaches 10 sites. (b) A snapshot of the CBPD order from the Monte Carlo simulations.

temperature disordered phase. Let us note that, for the nature of sMC, this phase diagram is most reliable away from the highly-quantum (low-temperature) regime.

In order to determine the transition (or crossover) lines in Fig. 4, we calculate the correlation lengths [16, 23] $\xi(\mathbf{q}) = |\delta\mathbf{q}|^{-1} \sqrt{[\mathcal{S}(\mathbf{q})/\mathcal{S}(\mathbf{q} + \delta\mathbf{q})] - 1}$, where $\mathcal{S}(\mathbf{q})$ is the structure factor for wave vector \mathbf{q} and $\delta\mathbf{q} = (2\pi/L, 0)$. We use $\mathcal{S}^{\text{SU}(2)}(\mathbf{q}) = \sum_{\mu=1}^3 \left\langle \left| \sum_i \hat{\lambda}_{\mu,i} e^{i\mathbf{q} \cdot \mathbf{r}_i} \right|^2 / L^2 \right\rangle$ and $\mathcal{S}^{\text{U}(1)}(\mathbf{q}) = \left\langle \left| \sum_i \hat{\lambda}_{8,i} e^{i\mathbf{q} \cdot \mathbf{r}_i} \right|^2 / L^2 \right\rangle$ to detect the correlations in the SU(2) and U(1) sectors, respectively. The R-B Néel and MUCN phases can be identified by $\mathcal{S}^{\text{SU}(2)}(\mathbf{q})$ with ordering vectors $\mathbf{q} = \mathbf{Q}_2 \equiv (\pi, \pi)$ and $\mathbf{q} = \mathbf{0}$, respectively. We confirm that there is no crossing point of $\xi^{\text{SU}(2)}/L$ for different system sizes down to low temperatures [see a typical case in Fig. 4(a)], which indicates no long-range order at $T > 0$ as expected. In Fig. 3, we plot the crossover temperature T_c^* from disordered to short-range correlated state by choosing the condition $\xi^{\text{SU}(2)} = 10$ sites [see Fig. 4(b)], which is comparable to the linear system size in typical cold-atom experiments in two dimensions [9].

The emergence of the nontrivial true long-range order between the regions with the R-B Néel and MUCN short-range correlations for $T > 0$ is of particular significance. In this phase, most of the snapshots in the sMC simulations show a checkerboard pattern where one sublattice is occupied mostly by $|G\rangle$ and the other by random superpositions of $|R\rangle$ and $|B\rangle$: $|\psi_{i_A}\rangle \simeq |G\rangle$, $|\psi_{i_B}\rangle \simeq \cos(\theta_{i_B}/2)|R_{i_B}\rangle + e^{i\phi_{i_B}} \sin(\theta_{i_B}/2)|B_{i_B}\rangle$, where θ_{i_B}, ϕ_{i_B} are randomly chosen at each site in each sMC snapshot (i.e., disordered in the SU(2) sector). This state breaks neither SU(2) nor U(1) symmetry, but *only the discrete translational symmetry*. Thus, the Mermin-

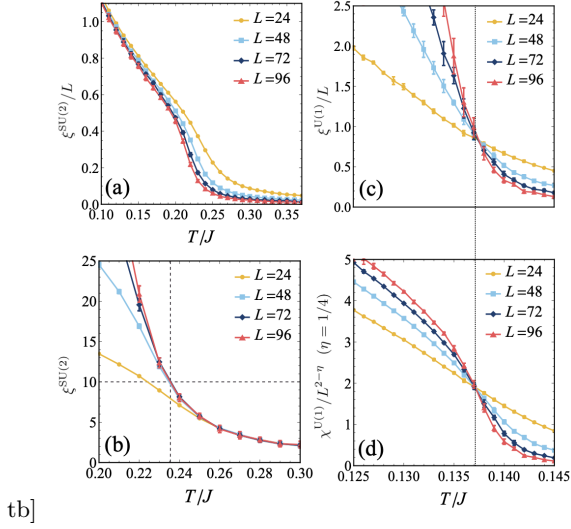


FIG. 4. Typical examples of the numerical data for the scaling analyses that obtain the finite-temperature phase diagram shown in Fig. 3. (a) scaled correlation length $\xi^{\text{SU}(2)}/L$ and (b) correlation length $\xi^{\text{SU}(2)}$ along $D/J = 2/\sqrt{3}$. (c) scaled correlation length and (b) scaled spin susceptibility with respect to λ_8 at $D/J = -1/2\sqrt{3}$.

Wagner-Hohenberg theorem [1, 2] does not forbid a finite-temperature phase transition to this “checkerboard partially disordered state” (CBPD) with true long-range order. In fact, as seen in Fig. 4(c), the scaled correlation lengths $\xi^{\text{U}(1)}/L$, obtained from $\mathcal{S}^{\text{U}(1)}(\mathbf{q} = \mathbf{Q}_2)$, for different linear sizes L cross each other at a certain critical point $T_c > 0$. According to the finite size scaling theory the scaled magnetic susceptibility $\chi^{\text{U}(1)}/L^{2-\eta}$, where $\chi^{\text{U}(1)} = (J/k_B T)\mathcal{S}^{\text{U}(1)}(\mathbf{Q}_2)$, should become size-independent at the critical temperature T_c : Fig. 4(d) shows that this scaling law is reproduced with critical exponent $\eta = 1/4$, indicating the 2D Ising universality class, as expected from the Z_2 translational symmetry breaking of the checkerboard pattern.

Let us discuss the mechanism of the emergence of CBPD order. Within the mean-field approximation, this phase is included in the infinitely degenerate ground-state manifold at the $\text{SU}(3)$ -symmetric point, since each pair of the \mathbf{d}_i vectors on neighboring sites is orthogonal. For $T > 0$ one sublattice is disordered in the $\text{SU}(2)$ sector while the checkerboard pattern is kept. Since the partial disorder compensates the loss of entropy, thermal fluctuations select this phase from the zero-temperature degenerate manifold. [24]

Experimental detection.— From an experimental perspective, it is convenient to describe the thermal phase diagram (Fig. 3) as a function of the global population imbalance P_g defined by $P_g = \sqrt{3} \sum_i \langle \hat{\lambda}_{8,i} \rangle = \frac{N_R + N_B - 2N_G}{N_R + N_B + N_G}$, where N_μ represents the global population of color μ [17], because this quantity, rather than D , is controllable in cold atom experiments [17]. Figure 5 shows the $T - P_g$

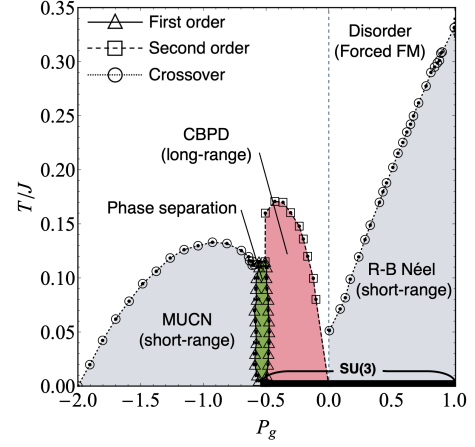


FIG. 5. Thermal phase diagram as a function of the population imbalance P_g . The thick horizontal line corresponds to the $\text{SU}(3)$ -symmetric point. Along that line, the variational solution is highly degenerate.

phase diagram. Note that a phase separation region appears between CBPD and MUCN. The detection of the CBPD order may be realized as follows. First, the $|\mathbf{G}\rangle$ state is removed from the entire lattice via optical pumping [21], then horizontal or vertical neighboring pairs of lattice sites are merged into single sites so as to form a new square lattice. At this point, signatures of the Mott insulating state, in which almost all sites are singly occupied by either R or B state, could be detected with the established techniques [25–27]; this would be proof of the realization of the CBPD order. In addition, the eventual extension of the quantum gas microscope technique to $\text{SU}(\mathcal{N})$ systems [28] could detect each phase more directly. Note that the sMC method replaces the statistics of discrete quantum levels by approximate continuous classical statistics of the vectors \mathbf{d}_i . Since this treatment should overestimate the entropy of paramagnetic states, thus underestimating the transition/crossover temperatures, the lines of $T_c(T_c^*)$ in Fig. 5 should be taken as lower bounds.

Conclusion.— We have investigated the emergence of long-range order by thermal disorder in the square-lattice $\text{SU}(3)$ Fermi gas at strong coupling with population imbalance and proposed experimental setups to realize and detect our predictions with alkaline-earth(-like) atoms. Applying mean-field theory and the sMC method to the $\text{SU}(3)$ Heisenberg model, we found that the competition between antiferromagnetic interactions and the population imbalance gives rise to several interesting magnetic states, including a true long-range ordered state that breaks only a discrete symmetry. This state enjoys an entropic advantage coming from the abundance of color degrees of freedom and is therefore favored by thermal fluctuations. This scenario generalizes the idea of emergent discrete symmetry breaking in low-dimensional sys-

tems without the traditional forms of magnetic frustration. Furthermore, we recall that the quantum fluctuations at $D = 0$ (no population imbalance) select the three-color stripe order, which should then persist for sufficiently small $D < 0$. This creates the condition for a finite-temperature transition originating from the difference between quantum and thermal order-by-disorder selection, a very rare phenomenon in magnetic systems [29, 30]; it would be worth investigating this aspect further, both experimentally and with theoretical methods that deal with quantum and thermal fluctuations simultaneously.

We would like to thank, Y. Takahashi, Y. Takasu and S. Taie, for useful discussions. This work was supported by JSPS KAKENHI Grant Nos. 18K03525 (DY), 21H05185 (GM, DY), 22H01171 (NF, DY), and JST PRESTO Grant No. JPMJPR2118, Japan (D.Y.)

* Corresponding author: yamamoto.daisuke21@nihon-u.ac.jp

- [1] P. C. Hohenberg, Phys. Rev. **158**, 383 (1967).
- [2] N. D. Mermin and H. Wagner, Phys. Rev. Lett. **17**, 1133 (1966).
- [3] P. Chandra, P. Coleman, and A. I. Larkin, Phys. Rev. Lett. **64**, 88 (1990).
- [4] C. Weber, L. Capriotti, G. Misguich, F. Becca, M. Elhajal, and F. Mila, Phys. Rev. Lett. **91**, 177202 (2003).
- [5] L. Capriotti, A. Fubini, T. Roscilde, and V. Tognetti, Phys. Rev. Lett. **92**, 157202 (2004).
- [6] O. Gauthé and F. Mila, Phys. Rev. Lett. **128**, 227202 (2022).
- [7] K. Karlová and J. Strečka, Solid State Communications **281**, 31 (2018).
- [8] K. Karlová and J. Strečka, Phase Transitions, A Multinational Journal **92**, 317 (2019).
- [9] A. Mazurenko, C. S. Chiu, G. Ji, M. F. Parsons, M. Kanász-Nagy, R. Schmidt, F. Grusdt, E. Demler, D. Greif, and M. Greiner, Nature (London) **545**, 462 (2017).
- [10] H. Kawamura and S. Miyashita, Journal of the Physical Society of Japan **53**, 4138 (1984).
- [11] M. A. Cazalilla and A. M. Rey, Reports on Progress in Physics **77**, 124401 (2014).
- [12] Y. Takahashi, Proceedings of the Japan Academy, Series B **98**, 141 (2022).
- [13] T. A. Tóth, A. M. Läuchli, F. Mila, and K. Penc, Phys. Rev. Lett. **105**, 265301 (2010).
- [14] B. Bauer, P. Corboz, A. M. Läuchli, L. Messio, K. Penc, M. Troyer, and F. Mila, Phys. Rev. B **85**, 125116 (2012).
- [15] P. Corboz, A. M. Läuchli, K. Penc, M. Troyer, and F. Mila, Phys. Rev. Lett. **107**, 215301 (2011).
- [16] D. Yamamoto, C. Suzuki, G. Marmorini, S. Okazaki, and N. Furukawa, Phys. Rev. Lett. **125**, 057204 (2020).
- [17] P. T. Brown, D. Mitra, E. Guardado-Sanchez, P. Schauß, S. S. Kondov, E. Khatami, T. Paiva, N. Trivedi, D. A. Huse, and W. S. Bakr, Science **357**, 1385 (2017).
- [18] M. Gell-Mann, Phys. Rev. **125**, 1067 (1962).
- [19] A. Läuchli, F. Mila, and K. Penc, Phys. Rev. Lett. **97**, 087205 (2006).
- [20] H. Tsunetsugu and M. Arikawa, Journal of the Physical Society of Japan **75**, 083701 (2006).
- [21] S. Taie, Y. Takasu, S. Sugawa, R. Yamazaki, T. Tsujimoto, R. Murakami, and Y. Takahashi, Phys. Rev. Lett. **105**, 190401 (2010).
- [22] E. M. Stoudenmire, S. Trebst, and L. Balents, Phys. Rev. B **79**, 214436 (2009).
- [23] L. Seabra, T. Momoi, P. Sindzingre, and N. Shannon, Phys. Rev. B **84**, 214418 (2011).
- [24] We conjecture that this argument should be true also for $\mathcal{N} > 3$, that is the $SU(\mathcal{N})$ Heisenberg model with $-D \sum_i \hat{\lambda}_{\mathcal{N}^2-1,i}$ field term.
- [25] R. Jördens, N. Strohmaier, K. Günter, H. Moritz, and T. Esslinger, Nature (London) **455**, 204 (2008).
- [26] J. F. Sherson, C. Weitenberg, M. Endres, M. Cheneau, I. Bloch, and S. Kuhr, Nature (London) **467**, 68 (2010).
- [27] D. Greif, L. Tarruell, T. Uehlinger, R. Jördens, and T. Esslinger, Phys. Rev. Lett. **106**, 145302 (2011).
- [28] D. Okuno, Y. Amano, K. Enomoto, N. Takei, and Y. Takahashi, New Journal of Physics **22**, 013041 (2020).
- [29] Q. Sheng and C. L. Henley, Journal of Physics: Condensed Matter **4**, 2937 (1992).
- [30] D. Yamamoto, G. Marmorini, M. Tabata, K. Sakakura, and I. Danshita, Phys. Rev. B **100**, 140410(R) (2019).